ELSEVIER

Journal of Alloys and Compounds 262–263 (1997) 194–197

Journal of ALLOYS AND COMPOUNDS

Hydrogen insertion effects on the structural and the magnetic properties of the $RFe_{10.5}Mo_{1.5}$ compounds (R = rare-earth metals)

E. Tomey[a,b,1], M. Bacmann[a], D. Fruchart[a,*], D. Gignoux[c], J.L. Soubeyroux[a]

[a] *Laboratoire de Cristallographie, CNRS, BP 166, 38042 Grenoble Cédex 9, France*
[b] *Instituto de Ciencia de Materiales de Aragon, CSIC, 50009, Zaragoza, Spain*
[c] *Laboratoire de Magnétisme L. Néel, CNRS, BP 166, 38042 Grenoble Cédex 9, France*

Abstract

The structural and magnetic properties of the $RFe_{10.5}Mo_{1.5}$ alloys and their hydrided derivatives have been extensively studied using X-ray, neutron diffraction and magnetic measurements. In this paper we discuss the impact of hydrogen insertion on the fundamental magnetic characteristics such as magnetisation, exchange couplings and magnetocrystalline anisotropy. © 1997 Elsevier Science S.A.

Keywords: Ferromagnetic alloys; Magnet materials; Exchange interactions; Anisotropy; Magnetic hydrides

1. Introduction

$R_2M_{14}B$, R_2M_{17} and $R(M,M')_{12}$ alloys, with R = rare earth and M,M' = transition metals have potential hard magnet properties when M = Fe and Co. Their structures exhibit interstitial sites in which atoms of small size can be inserted. Most of the alloy fundamental characteristics are dramatically modified by such an insertion of a light element. The Curie temperature and the local magnetic moments on the iron sites depend on the volume expansion, and the magnetocrystalline anisotropy of the R element depends on the charge density distribution in its neighbourhood. In a previous paper we reported on structural and magnetic properties before and after hydrogen insertion in the $RFe_{10.5}Mo_{1.5}H_x$ series. At the light of these experimental results we will examine some features of the models used to better understand the changes induced in fundamental properties.

2. Experimental and results

Extended details on the alloys synthesis, the hydrogenation procedure, the crystal structure determination (using X-ray and neutron diffraction techniques), the bulk magnetisation measurements on free and oriented samples, AC susceptibility measurements were reported in a previous paper [1].

All samples were found to crystallise in the $ThMn_{12}$-type of structure (space group I4/mmm; $Z = 2$). Rare-earth atoms occupy the 2a site whereas iron atoms occupy the three sites 8f, 8i and 8j. The molybdenum atom preferentially occupies the 8i site. Hydrogen atoms occupy the 2b site, with a maximum of one interstitial atom per formula unit.

The cell parameters of the alloys follow different trends along the rare-earth series. The *a* parameter

* Corresponding author.
[1] Present address: ARELEC SA BP 429 Pau Cedex, France.

0925-8388/97/$17.00
PII S0925-8388(97)00379-4

decreases linearly from R = Pr to R = Lu. The c parameter remains almost constant as a function of the number of 4f electrons. Along the R series, the behaviour of the c/a ratio shows a continuous increase towards an asymptotic value for the heaviest rare-earth elements. Upon hydrogen uptake, the relative volume increase ranges from 1.3% (R = Sm) to 0.4% (R = Gd). Both a and c cell parameters decrease linearly with the number of 4f electron of R. The decrease in c remains slight and that in a is less pronounced than in the corresponding alloys.

The Curie temperature T_C of the starting alloys ranges between 460 K (R = Gd) and 335 K (R = Ce). Its variation agrees well with de Gennes' factor $G_J = (g_J - 1)^2 J(J+1)$ for the rare-earth element. The magnetisation values account for the well-known antiferromagnetic interaction between R and 3d spins, giving rise to ferromagnetic couplings for the light rare-earth elements and ferrimagnetic arrangements for the heavy ones. For the alloys with non-magnetic R elements (Y or Lu), the magnetic moments are aligned along the c axis below T_C. When R is a magnetic element, anomalies in the AC-susceptibility and magnetisation vs. temperature curves can be interpreted in most cases as the result of spin reorientation transitions (SRT). Iron appears as favouring an easy axis behaviour, but depending on the sign of the second order Stevens' coefficient α_J, the R-magnetocrystalline anisotropy favours an easy-axis ($\alpha_J > 0$) behaviour or an easy-plane one ($\alpha_J < 0$). However, with Er ($\alpha_J > 0$) a SRT is observed at low temperature.

The Curie temperatures are increased upon hydrogen insertion, and values range between 430 K (R = Tm) and 500 K (R = Gd). The relative Curie temperature increase ($\Delta T_C/T_C$) upon hydrogen insertion is minimum for R = Gd, whereas the de Gennes' factor is still verified even although strongly attenuated. At 4 K and for the R based non-magnetic element the saturation magnetisation is increased by $\Delta M_S = 0.5$ μ_B/f.u. The situation revealed by neutron powder diffraction is more complicated. At low temperature in the $ErFe_{10.5}Mo_{1.5}D_x$ system, the magnetic moment on the 8i and 8f iron sites is found to increase whereas that on the 8j iron position decreases upon hydrogenation. The 4f–5d–3d exchange coupling scheme is verified along the hydrides series.

As for the host alloys, the hydrides with a non-magnetic R element have a c-easy axis behaviour in the whole temperature range. In most cases and for R($\alpha_J < 0$)-based starting alloys that exhibit an easy plane or a tilted structure at low temperature, upon hydrogen insertion one observes an increase of the temperature range in which such structures are stabilised. On the contrary, the SRT of the Er($\alpha_J > 0$)-based alloy is decreased upon hydrogen insertion.

The results concerning the magnetic phases diagrams are schematised in Fig. 1a,b for the host alloys and the corresponding hydrides, respectively.

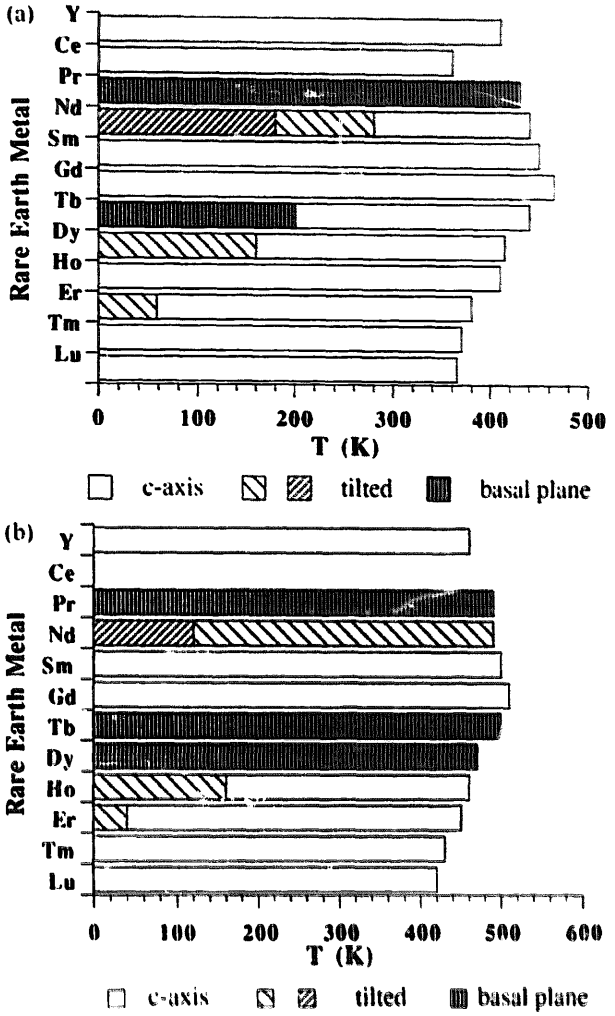

Fig. 1. (a) Magnetic phase diagram for the $RFe_{10.5}Mo_{1.5}$ alloys. (b) Magnetic phase diagram for the $RFe_{10.5}Mo_{1.5}H_{x\approx1}$ hydrides.

3. Discussion

The behaviour of the cell parameters vs. the R element indicates that the c parameter is mainly depending on the Kagomé lattice of the $ThMn_{12}$-type structure [planes ($\approx 1/4,0,0$)] while the a parameter expansion is directly governed by the atomic radius of the rare-earth element. The change in the c/a ratio upon hydrogenation indicates that, for large R atoms, the cell expansion is mainly governed by the H–R interatomic distance. For small R atoms, the change of the cell volume is also controlled by the distortion of the Kagomé lattice.

The Ce-based alloy differs from the general behaviour. In this alloy we calculated the mean radius of Ce atom to be $\langle r^{exp} \rangle = 1.78$ Å. On this basis, the behaviour of the Ce-based alloy can be interpreted as corresponding to a mixed valence cerium state [2]. We

have determined the valence V of Ce atom using the formula:

$$\langle r^{exp}\rangle = (1-\nu)\langle r^{+3}\rangle + \nu\langle r^{+4}\rangle; \quad V = 3+\nu \qquad (1)$$

In this expression the radii for the tetra- and trivalent cerium-states were taken from [3] and ν is the contribution of the tetravalent state. In the alloy the estimated value of the valence is 3.32(5), which agrees well with an X-ray spectroscopy determination $V=3.33(3)$ in the parent compound $CeFe_{11}Ti$ [4].

The effect of hydrogen insertion on the magnetisation of the 3d sublattices should be interpreted as the result of two main effects. The first one should be the narrowing of the 3d band induced by the cell volume increase which leads to an increase of the values of the magnetic moments on the iron atoms located at the 8i and 8f sites. The second one should be an electron transfer from hydrogen to the conduction metal bands. In term of 'local' picture, the latter effect may concern mainly the nearest-neighbours 8j iron. From spin-polarised band structure calculations, the density of states (DOS) at the Fermi level is higher for minus spin states [5] than for the opposite ones. Hence, in a rigid band model, the charge transfer would lead to a reduction of the magnetic moment at this site.

The Curie temperature increase originates from the combination of two effects, namely a weak mean magnetic moment increase and mostly the enhancement of Fe–Fe exchange interactions related with the volume expansion [6]. The behaviour of $\Delta T_C/T_C$ along the series results also from the decrease of R–Fe exchange coupling upon hydrogenation. Within the molecular field approximation and neglecting the R–R interaction the Curie temperature can be expressed as follows:

$$T_C = \frac{T_{Fe}}{2} + \sqrt{\left(\frac{T_{Fe}}{2}\right)^2 + \frac{16N_R N_{Fe}}{9K_B^2} n_{R-Fe}^2 S(S+1)\mu_B^4 G_j} \qquad (2)$$

and

$$T_{Fe} = \frac{4N_{Fe}}{3K_B} n_{Fe}\mu_B^2 S(S+1) \qquad (3)$$

where N_i is the i-sublattice number of atoms in the unit cell, G_j is the above mentioned de Gennes' factor, μ_B is the Bohr magneton, S is the effective spin of the iron sublattice as defined by $m_{Fe} = -2\mu_B S$ and m_{Fe} is the mean magnetic moment of iron at low temperature. The molecular field parameters are related to the standard interatomic exchange coupling terms by the expressions [7]:

$$n_{Fe} = \frac{Z_{FeFe}}{2N_{Fe}\mu_B^2} J_{FeFe} \qquad (4)$$

$$n_{R-Fe}^2 = \frac{Z_{RFe}Z_{FeR}}{16N_R N_{Fe}\mu_B^4} J_{RFe}^2 \qquad (5)$$

where Z_{AB} is the number of B first neighbours around the A atom.

Table 1
Parameters of the fit of the T_C to the experimental values according to Eq. (1)

Series	R elements	T_{Fe} (K)	$\frac{16N_R N_{Fe}}{9K_B^2} n_{R-Fe}^2 S(S+1)$ $\mu_B^4(10^2K^2)$
Alloys	Light	412 ± 6	37 ± 12
	Heavy	360 ± 6	30 ± 4
Hydrides	Light	462 ± 6	32 ± 10
	Heavy	426 ± 6	25 ± 3

Fitting the experimental T_C values to Eq. (2), the experimental dots are found to belong to two separate branches, one for the light rare-earth elements and another for the heavy ones. The corresponding values are shown in Table 1.

These results show that:

1. The 3d contribution to the Curie temperature markedly increases upon hydrogen insertion. As mentioned above, this behaviour is related with the distance dependence of the Fe–Fe exchange interaction as proposed by Néel [6]. To quantify this effect, the Fe magnetic moment increase upon hydrogenation should be taken into account as well.
2. The initial (alloy) and final (hydride) 3d contribution to T_C is also governed by the lanthanide contraction vs. the number of 4f electrons [8]. In fact, this effect shows again the dependence of the Fe–Fe interactions on the distance but also for a part on the size of the R element.
3. The two-branches-like contribution of the R-transition metal interaction to the ordering temperature decreases upon the hydrogen uptake. This has been already discussed for the $R_2Fe_{17}H_x$ series [9,10]. It has been attributed to the decrease of the exchange coupling terms J_{RFe}. This 4f–3d exchange term, through the 5d electrons, should diminish because of the reduction of the 4f–5d orbital overlapping related to the cell expansion.

The rare-earth sublattice anisotropy arises from the crystal electric field (CEF) [11]. As found by means of single crystal analysis [12,13], the second order CEF parameter A_2^0 is negative and small in magnitude. Hence, it favours an easy magnetisation direction (EMD) along and perpendicular to c, for R with second order Steven's factor $\alpha_J > 0$ (e.g. Sm) and $\alpha_J < 0$ (e.g. Pr), respectively. The competition between the 3d and the rare-earth magnetocrystalline anisotropies gives rise to SRTs (e.g. Tb). The SRT observed in the Nd, Dy and Er compounds can be understood by taking into account higher order terms of the CEF hamiltonian. Upon the hydrogenation process, because of the modification on the quadrupolar term, the A_2^0 parameter remains negative but is strongly increased in magnitude. As a consequence, the above mentioned contribution of rare-earth elements to the magnetocrystalline anisotropy is enhanced. Hence, at room temperature Tb and Dy-based hydrides have their magnetic moments lying in the basal plane, the Ho hydride undergoes a SRT around 200 K and in Nd-based hydride, the canting from the c axis is increased. A donor character of hydrogen confirms the Coehoorn's picture and the relative importance of the valence electron contribution to the second order crystal field parameter [14]. When the second order Stevens' coefficient α_J is negative, hydrogen insertion along the axial R–H–R environment reinforces the R contribution to the magnetocrystalline anisotropy and reciprocally for positive α_J. As shown in Fig. 2 this leads to an enhancement of the prolate character of the 4f shell and accordingly of the magnitude of the A_2^0 parameter that remains negative.

4. Conclusion

Hydrogen insertion leads to: (i) an anisotropic expansion of the lattice along the R series; (ii) an increase of the ordering temperature (up to ≈ 15%); and (iii) a weak increase of magnetisation. The A_2^0 parameter remains negative but strongly increases in magnitude. From these considerations the Sm-based hydride of the $ThMn_{12}$-type of structure appears as a possible candidate to be used as starting materials in the manufacture of rare-earth permanent magnets.

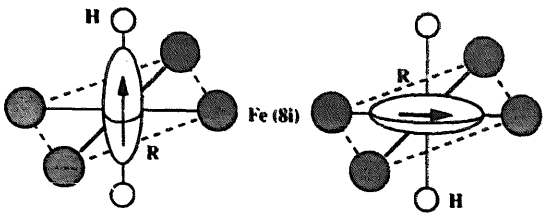

Fig. 2. Schematised diagram that mimics the influence of hydrogen on the rare-earth 4f shell. Arrows indicate the direction of the magnetic moments for rare-earth atoms: (a) left: Sm-like ($\alpha_J > 0$); (b) right: Nd-like ($\alpha_J < 0$).

Acknowledgement

One of us (ET) thanks the BRITE/EURAM 4393-90 contract for financial support.

References

[1] E. Tomey, M. Bacmann, D. Fruchart, J.L. Soubeyroux, D. Gignoux, J. Alloys Comp. 231 (1995) 195.
[2] J. Röhler, in: K.A. Gschneidner, L. Eyring, S. Hüfner (Eds.), Handbook on the Physics and the Chemistry of Rare Earths, Vol. 10, North-Holland, 1987.
[3] E.T. Teatum, K.A. Gschneidner, J.T. Waber, Los Alamos Scientific Laboratory, Report L.A. 4003, 1968.
[4] J. Chaboy, A. Marcelli, L. Bozukov, et al., Phys. Rev. B 51 (1995) 9005.
[5] S. Ishida, S. Asano, S. Fujii, Physica B 193 (1994) 66–76.
[6] L. Néel, Ann. Phys. 5 (1932) 232.
[7] J.F. Herbst, Rev. Mod. Phys. 63 (1991) 819–898.
[8] W.E. Wallace, Prog. Solid State Chem. 16 (1985) 127.
[9] O. Isnard, PhD Thesis, University of Grenoble, France, 1993.
[10] D. Fruchart, O. Isnard, S. Miraglia, J.L. Soubeyroux, J. Alloys Comp. 231 (1995) 188.
[11] M.T. Hutchings, in: F. Seitz, D. Turnbull (Eds.), Solid State Physic, Vol. 16, Academic Press, 1964.
[12] B.P. Hu, H.S. Li, J.M.D. Coey, J.P. Gavigan, Phys. Rev. B 41 (1990) 2221–2228.
[13] E. Tomey et al., PhD Thesis, University of Grenoble, France, 1994.
[14] R. Coehoorn, II Ciocco NATO Summer School 1990, ASI, Kluwer Acad. Pub. 1992, p. 331.